Distance Estimation From a Diffusive Process: Theoretical Limits and Experimental Results

Fabio Broghammer, Siwei Zhang, *Member, IEEE*, Thomas Wiedemann, and Peter A. Hoeher, *Fellow, IEEE*

***Abstract*—Estimating the distance between the source of a diffusive process and a receiver has a variety of applications, ranging from gas source localization at the macro-scale to molecular communication at the micro-scale. Distance information can be extracted from features of the observed particle concentration, e.g., its peak. This paper derives the Cramér-Rao lower bound (CRB) for distance estimation given the advection-diffusion model for absorbing receivers, which is the fundamental limit of any distance estimator. Furthermore, CRBs are obtained for estimators using only information about the observed peak. A maximum-likelihood estimator using the entire signal and two estimators based on peak detection are deduced. The derived CRBs are used to study the effect of channel parameters on the estimation performance. Finally, the performance of the proposed estimators is verified by comparing the root mean squared errors with their theoretical bounds in a simulation, and preliminary experimental results are presented.**

***Index Terms*—Cramér-Rao lower bound, molecular communication, molecular localization, parameter estimation, ranging.**

I. Introduction

LOCALIZING the source of a diffusive process is an important feature in many fields, including gas source localization and molecular communication (MC). In disaster scenarios, e.g., the leakage of a toxic gas, the gas diffuses into the environment, where it is also affected by advection. In such scenarios, it is important to find the gas source quickly. Due to the high dangers to humans, research is being conducted on gas source localization using robotic swarms [1]. The swarm allows the estimation of the distances to the source from different vantage points. When this distance information is fused, the source can be easily localized. Another application where diffusive processes occur is MC. In MC, information is transmitted by molecules emitted into the environment and transported by diffusion mechanisms and drift. An example at the micro-scale is the human blood circulatory system. Many applications in micro-scale, such as targeted drug delivery and human body health monitoring, would benefit from the position-awareness of MC senders and receivers. MC can also be applied on a macro-scale with larger distances [2]. Examples include pipe and duct systems, where conventional communication schemes fail [3]. In all applications, distance estimation is an essential ingredient for localization and thus for position-awareness.

Distance estimation using observations from a diffusive process receives a lot of attention, especially in the field of MC, as the channel between the transmitter and receiver depends on the distance. The methods used for distance estimation, such as round trip time [4], signal attenuation [4] and time difference of arrival [5], are known from radio localization. For diffusive channels with absorbing receivers, a maximum likelihood (ML) distance estimator is derived in [6]. However, the effect of the channel parameters on the distance performance is only examined simulatively and no theoretical limits are derived. In [7], a ML distance estimator and the Cramér-Rao lower bound (CRB) for transparent receivers are derived. Furthermore, the ML estimator and the CRB are compared to other estimation approaches in simulation. Nevertheless, no performance bounds have been derived for other estimation approaches, such as peak-based approaches, so a theoretical analysis of the effect of channel parameters is not yet possible. For diffusive channels with inter-symbol interference, a theoretical limit is derived in [8], which is an important step towards joint communication and distance estimation. Other works on communication do not estimate individual channel parameters, such as distance, but the total channel impulse response directly based on known transmitted signals [9]. Overall, there is also a lack of experimental evaluations of the models.

In this paper, we study the limits of different distance estimation approaches based on a one-dimensional (1D) advection-diffusion channel with an absorbing receiver. For the theoretical analysis of the estimation performance, we use CRBs. The CRB is a lower bound for the variance of any unbiased estimator [10]. Thus, the bound is suitable for comparing different estimation approaches independently of concrete estimators and enables assessing the performance of a concrete estimator. In addition, the effect of the channel parameters on the estimator performance can be studied. The primary contributions of this paper can be summarized as follows:

- We derive the CRB for the ML distance estimator presented in [6]. This bound provides the fundamental limit of any distance estimator.
- Based on approximated distributions of the observed time of peak concentrations (ToPCs) and amplitude of peak concentrations (AoPCs), we derive CRBs for distance

Manuscript received 28 April 2023; revised 21 July 2023; accepted 31 July 2023. Date of publication 8 August 2023; date of current version 20 September 2023. The associate editor coordinating the review of this article and approving it for publication was V. Jamali. *(Corresponding author: Fabio Broghammer.)*

Fabio Broghammer, Siwei Zhang, and Thomas Wiedemann are with the Institute of Communications and Navigation, German Aerospace Center, 82234 Weßling, Germany (e-mail: fabio.broghammer@dlr.de).

Peter A. Hoeher is with the Faculty of Engineering, Kiel University, 24118 Kiel, Germany.

Digital Object Identifier 10.1109/TMBMC.2023.3303363

estimators which use only information about the ToPC or the AoPC.
- We study the effect of channel parameters on the estimation performance of different estimation approaches. Furthermore, we compare the derived CRBs together with concrete estimators in a simulation.
- We present our experimental setup and preliminary experimental results.

II. Theoretical Analysis and Limitations

In this section, we describe the used particle dispersion model and derive CRBs for various distance estimators which use different observations of the received signal.

A. System Model

We consider a 1D advection-diffusion environment with a source and a receiver. It is assumed that source and receiver are time-synchronized and that the particles are absorbed at the receiver. The source emits C particles at time $t = 0$ s. All particles are emitted at the same time as an impulse. The particles diffuse according to a Brownian motion which is superimposed with a constant drift. Brownian motion describes the random motion of a particle in a fluid.

The receiver is located at a distance of d from the source in the drift direction. Since the motion of a particle is affected by a random motion, the arrival time t_i of the i-th particle at the receiver is a random variable. The distribution of t_i is described by the parameterized probability density function (PDF) [11]

$$p(t_i; d) = \frac{d}{\sqrt{4\pi D t_i^3}} \exp\left(- \frac{(d - v t_i)^2}{4 D t_i} \right), \quad t_i > 0, \quad (1)$$

where D is the diffusion coefficient, v the drift velocity and d the distance between the source and the receiver. This PDF belongs to an inverse Gaussian distribution with mean $\mu = \frac{d}{v}$ and shape parameter $\lambda = \frac{d^2}{2D}$ [12]. Multiplying the PDF (1) by the number of emitted particles C gives the expected concentration over time $\bar{c}(t) = C p(t; d)$ at the receiver. Since the source emits an impulse, $\bar{c}(t)$ can also be seen as the channel impulse response (CIR) [9], [13].

B. Theoretical Limit of Estimation Performance

To investigate the theoretical limits of distance estimation performance using diffusive processes, we derive the CRB based on the distribution of arrival times (1) without considering other effects such as sensor noise. We assume that the arrival times $t_1, \ldots, t_C$ of all particles can be observed. Since $t_1, \ldots, t_C$ are independent and identically distributed samples of the PDF (1), we can calculate the joint PDF as

$$p(t_1, \ldots, t_C; d) = \prod_{i=1}^{C} p(t_i; d). \quad (2)$$

With $\mathbb{E}_{t;d}[t^{-1}] = \mu^{-1} + \lambda^{-1}$ [12], it is straightforward to verify that the regularity condition of the CRB, $\mathbb{E}_{t;d}[\frac{\partial}{\partial d} \ln p(t_1, \ldots, t_C; d)] = 0$, is met and thus the CRB exists. $\mathbb{E}_{t;d}$ is the expectation taken with respect to $p(t; d)$. The CRB is given by

$$\mathrm{CRB}(d) = -\mathbb{E}_{t;d}\left[\frac{\partial^2}{\partial d^2} \ln \prod_{i=1}^{C} p(t_i; d) \right]^{-1} = \frac{1}{C} \frac{2Dd^2}{4D + vd}. \quad (3)$$

Since we used (1) and all available information without further disturbances to calculate (3), the CRB represents the theoretical limit of distance estimation performance exploiting observations of diffusive processes.

In the next two sections, we derive CRBs for estimators which only use the ToPC or the AoPC to estimate the distance to the source, respectively.

C. CRB for ToPC Based Estimators

Due to the stochastic nature of the Brownian motion and the limited number of particles, the ToPC t_{peak} is a random variable with PDF $p(t_{\mathrm{peak}}; d)$. The CRB is then given by

$$\mathrm{CRB}_{\mathrm{ToPC}}(d) = -\mathbb{E}_{t_{\mathrm{peak}};d}\left[\frac{\partial^2}{\partial d^2} \ln p\big(t_{\mathrm{peak}}; d\big) \right]^{-1} \quad (4)$$

if the regularity condition is satisfied. Since the closed form of the PDF $p(t_{\mathrm{peak}}; d)$ cannot be easily determined, we will derive a CRB based on an approximation of $p(t_{\mathrm{peak}}; d)$. This "approximated" CRB then depends on the approximation used and is therefore not a true lower bound for the original estimation problem. But as shown in Section IV, the "approximated" CRB can be used to compare the influence of the distance to the different estimation approaches. As an approximation for $p(t_{\mathrm{peak}}; d)$, we use a Gaussian distribution $\mathcal{N}(\mu, \sigma^2)$ which is described by the expected value μ and the variance σ^2. Using $\bar{c}(t)$, the expected ToPC $\bar{t}_{\mathrm{peak}}$ can be written (cf. [7], [12]) as

$$\bar{t}_{\mathrm{peak}}(d) = \arg\max_t \ \bar{c}(t) = \frac{1}{v}\left[\sqrt{d^2 + 9\frac{D^2}{v^2}} - 3\frac{D}{v} \right]. \quad (5)$$

For the variance, we use Monte Carlo simulation with 10^4 runs as presented in Section IV. For every distance d, we evaluate the sample variance σ_d^2 of the observed realizations of t_{peak}. Finally, we can approximate $p(t_{\mathrm{peak}}; d) \approx \mathcal{N}(\bar{t}_{\mathrm{peak}}(d), \sigma_d^2)$. An example for $d = 4$ m can be found in Fig. 1.

With this approximation, the CRB for the Gaussian distribution [10] and the chain rule for the derivative of composite functions, the CRB based on the approximation is given by

$$\widetilde{\mathrm{CRB}}_{\mathrm{ToPC}}(d) = \frac{\sigma_d^2}{\left(\frac{\partial}{\partial d}\bar{t}_{\mathrm{peak}}(d)\right)^2} = \frac{(9D^2 + v^2 d^2)\sigma_d^2}{d^2}. \quad (6)$$

Remark 1: For each distance d a variance σ_d^2 is calculated, which is also used in the evaluation in Section IV. However, when calculating the bound, the variance is assumed to be constant over the distance, as otherwise the bound would take information regarding the shape of the observed signal into account in addition to the information from the ToPC. Since a ToPC based estimator uses only the observed ToPC, but no information about the shape, the comparison would otherwise be skewed and unjustified.

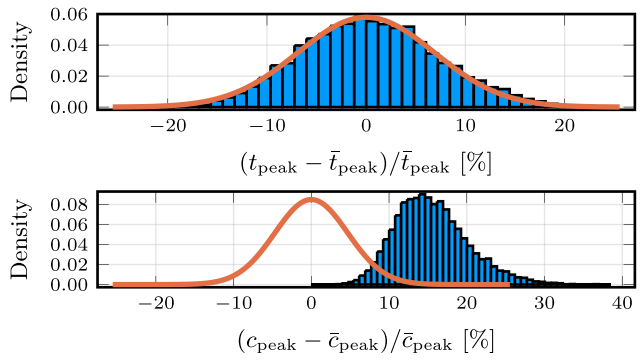

Fig. 1. Normalized distributions of the observed ToPC t_{peak} (upper plot) and AoPC c_{peak} (lower plot) relative to the expected values $\bar{t}_{\text{peak}}$ and $\bar{c}_{\text{peak}}$ for 10^4 Monte Carlo runs and a distance of $d = 4$ m. The other parameters were chosen as in Section IV. The orange lines show the Gaussian approximation. In the lower plot, the bias of the observed AoPCs is clearly shown.

D. CRB for AoPC Based Estimators

As in Section II-C, the AoPC is also affected by the stochasticity introduced by the Brownian motion and the limited number of particles. Again, the true PDF $p(c_{\text{peak}}; d)$ cannot be easily determined. To approximate the PDF, we use the same approach as described in Section II-C. The expected AoPC is given by inserting (5) into $\bar{c}(t)$:

$$\bar{c}_{\text{peak}}(d) = \frac{Cd}{\sqrt{4\pi D\left(\bar{t}_{\text{peak}}(d)\right)^3}} \exp\left(-\frac{\left(d - v\bar{t}_{\text{peak}}(d)\right)^2}{4D\bar{t}_{\text{peak}}(d)}\right). \tag{7}$$

Unlike in Section II-C, the statistic of c_{peak} observed in the simulation is biased because we take the maximum amplitude of the noisy concentration signal (cf. Fig. 1). Nevertheless, in order to evaluate the performance of an AoPC estimator with a CRB, we consider only the variance of the observed statistic and approximate the PDF by $p(c_{\text{peak}}; d) \approx \mathcal{N}(\bar{c}_{\text{peak}}(d), \tilde{\sigma}_d^2)$, where $\tilde{\sigma}_d^2$ is the sample variance obtained in simulation (see Fig. 1). The CRB based on the approximation is given by

$$\widetilde{\text{CRB}}_{\text{AoPC}}(d) = \frac{\tilde{\sigma}_d^2}{\left(\frac{\partial}{\partial d}\bar{c}_{\text{peak}}(d)\right)^2}. \tag{8}$$

Because of the bias, the obtained CRB is not a bound, not even for the approximated estimation problem, but still gives insights for comparing estimator performances [7]. Due to space limitations, the equation is not simplified further.

E. Effect of Channel Parameters on Estimation Performance

In this section, we study the effect of the channel parameters on the different estimation approaches.

From the theoretical limit (3), it can be seen that the estimation performance increases (the bound decreases) with a increasing number of particles. The same observation can be made for the drift velocity v. As v increases, the particles have less time to diffuse. Since the transmitted impulse becomes less blurred, the estimation performance increases. For $v \to 0$ the estimation performance is proportional to the squared distance d^2. Since we only consider the noise introduced by the Brownian motion (diffusion), the estimation performance increases as the effect of diffusion D decreases. Without noise ($D = 0$) the distance can be calculated perfectly. For $D \to \infty$, the bound is proportional to d^2.

For the ToPC based approaches, the analysis is not so trivial because σ_d^2 in (6) also depends on the channel parameters. Numerical evaluations have shown that we can choose σ_d^2 arbitrarily, since the number of particles C only affects σ_d^2. For this reason, we ignore the influence of the other parameters on σ_d^2, since they can be compensated by C. Intuitively, the estimation performance of a ToPC based estimator increases as the difference between peak times for different distances increases. This explains why, in contrast to (3), distance estimation performance decreases with increasing drift velocity v (v^2 in the numerator). As for the theoretical limit, the estimation performance also decreases with a stronger diffusion influence. The analysis of AoPC based estimators is analogous, but is not presented due to space limitations.

III. Distance Estimators

In this section, we introduce an estimator for each CRB presented in Section II. The first estimator is a ML estimator using the full signal's information. The other two estimators use the ToPC and the AoPC, respectively, to estimate the distance. Thus, only the time of the maximum concentration or the maximum concentration itself need to be observed, which significantly simplifies the practical implementation of the estimators.

A. ML Estimator

With (2), the ML estimator is defined by

$$\hat{d}_{\text{ML}} = \arg\max_d \; p(t_1, \ldots, t_C; d). \tag{9}$$

A closed form solution is derived in [6]:

$$\hat{d}_{\text{ML}} = \frac{v}{2\overline{f}} + \sqrt{\frac{v^2}{4\overline{f}^2} + \frac{2D}{\overline{f}}}, \text{with}\, \overline{f} := \frac{1}{C}\sum_{i=1}^{C}\frac{1}{t_i}. \tag{10}$$

For a large number of particles, $\overline{f}$ can be approximated by $\overline{f} \approx \frac{1}{C}\int \frac{1}{t}c(t)\,dt$, where $c(t)$ is the observed concentration.

B. ToPC Based Estimator

The ToPC based estimator uses only the observed ToPC t_{peak} to estimate the distance. Thus, the estimator does not need to know how many particles were emitted. The estimator

$$\hat{d}_{\text{ToPC}} = \sqrt{v^2 {t_{\text{peak}}}^2 + 6Dt_{\text{peak}}} \tag{11}$$

is obtained by solving (5) for the distance d and substituting the expected for the observed ToPC.

C. AoPC Based Estimator

For the AoPC estimator, the expected AoPC $\bar{c}_{\text{peak}}$ in (7) is replaced by the observed AoPC c_{peak}:

$$c_{\text{peak}}(d) = \frac{Cd}{\sqrt{4\pi D\left(\bar{t}_{\text{peak}}(d)\right)^3}} \exp\left(-\frac{\left(d - v\bar{t}_{\text{peak}}(d)\right)^2}{4D\bar{t}_{\text{peak}}(d)}\right). \tag{12}$$

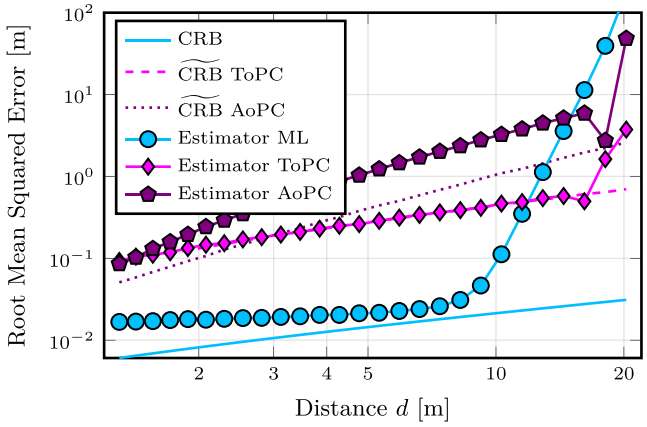

Fig. 2. Simulation results for the CRBs and estimators presented in Section II and Section III, respectively, over 10^3 Monte Carlo runs. The parameters were chosen as drift velocity $v = 0.4\,\mathrm{m\,s^{-1}}$ and diffusion constant $D = 0.1\,\mathrm{m^2\,s^{-1}}$. The diffusive process was observed for 40 s.

Because of the complexity of the expression, no closed-form solution was found for the estimator. Eq. (12) is however bijective, so a unique solution for the distance d can be found using a numerical root finding algorithm.

IV. Numerical Evaluation

To evaluate the theoretical results, we use a numerical simulation. In the simulation, the Brownian motion of $C = 10^4$ individual particles is simulated according to

$$\begin{aligned} x_i(0) &= 0 \\ x_i(t+\Delta t) &= x_i(t) + v\,\Delta t + \phi_i(t), \quad \forall i = 1,\dots,C, \end{aligned} \tag{13}$$

with $\phi_i(t) \sim \mathcal{N}(0, 2D\Delta t)$. The time between simulation steps is chosen as $\Delta t = 10^{-3}$ s to obtain a high temporal resolution. The arrival times $t_1,\dots,t_C$ of the particles are determined by checking when each particle arrives for the first time at distance d. To move from arrival times to a concentration over time, we generate a histogram with bin sizes of 0.1 s. Due to the limited number of particles C, the received concentration over time has a small signal-to-noise ratio. At any distance, the receiver observes the process for 40 s, starting with the gas release. For particles that do not arrive within the 40 s after they have been released from the source, we assume that they arrive at time $t = \infty$.

Fig. 2 shows the results for the CRBs introduced in Section II and the root mean squared errors (RMSEs) of the estimators introduced in Section III. All values are evaluated over 10^3 Monte Carlo runs.

The parameters used in the simulation are: drift velocity $v = 0.4\,\mathrm{m\,s^{-1}}$, diffusion coefficient $D = 0.1\,\mathrm{m^2\,s^{-1}}$ and particle count $C = 10^4$. The drift velocity and distances are chosen analogously to the values in the experiment in Section V. In order to highlight the effect of diffusion, the diffusion constant is chosen to be two orders of magnitude larger than the one observed in the experiment.

As expected, the theoretical limit (CRB) from Section II-B is a lower bound. The ML estimator performs close to the CRB. Further investigations have shown that the CRB can be reached by decreasing Δt. However, this leads to a higher computational cost of simulation. The ToPC based estimator

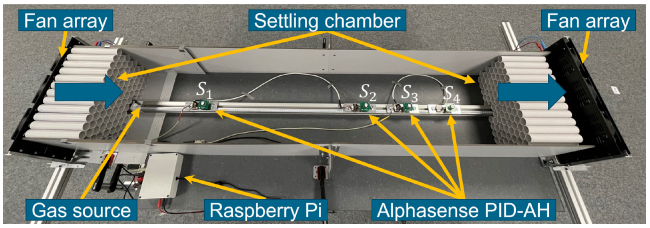

Fig. 3. The experimental setup is about 2 m long, 40 cm wide and 30 cm high. The blue arrows show the wind direction. The settling chambers are used to obtain laminar airflow. The gas source can be controlled by the Raspberry Pi. The entire setup is closed with a lid during operation.

reaches the CRB ($\widetilde{\text{CRB}}_{\text{ToPC}}$) which is based on the approximated distribution of t_{peak}. This fact shows that $\widetilde{\text{CRB}}_{\text{ToPC}}$ gives insights about the real estimation performance. As mentioned in Section II-D, the AoPC estimator is biased. Due to the noise on the concentration it is very likely that the observed maximum is higher than the amplitude expected by the channel model. Thus, the AoPC estimator underestimates the distance. Since the CRB is a lower bound for unbiased estimators, $\widetilde{\text{CRB}}_{\text{AoPC}}$ only provides insights for performance comparisons [7]. But it can be seen that the RMSE of the AoPC based estimator follows the same trend as $\widetilde{\text{CRB}}_{\text{AoPC}}$.

Comparing the ML estimator with the peak based estimators, one can see that exploiting more features of the concentration results in better estimator performance. For small distances, the "approximated" CRBs indicate that AoPC approaches can outperform ToPC based approaches. However, this changes for larger distances and ToPC estimators become better. This is most likely due to the smaller changes in amplitude at long distances. A similar effect can be observed in radio ranging when comparing estimators using the received signal strength with time of arrival estimators [14].

Since the process is only observed for 40 s, fewer particles arrive in time for longer distances. Thus, their arrival time is considered as $t = \infty$. As a result, the RMSE of the ML estimator increases. The peak leaves the 40 s time window later because it depends only on the arrival times around the peak concentration and not on the arrival times of the slow particles. Hence, the RMSEs of the ToPC and AoPC estimator are stable even for longer distances compared to the ML approach. The RMSE dips occur when the peak lies just after 40 s. The observed ToPC is then very likely at $t = 40$ s and the observed AoPC is lower, so the distance is no longer underestimated. For the ML estimator, there is no dip because the estimator uses the entire signal and for longer distances, the arrival time $t = \infty$ is assumed for more and more particles.

V. Experimental Evaluation

To evaluate the performance of the presented estimators in practice, we built a macro-scale experimental setup. Our experimental setup is inspired by a wind tunnel and shown in Fig. 3. The setup is about 2 m long, 40 cm wide and 30 cm high. Fan arrays on both sides generate an airflow in the channel with the direction indicated by the blue arrows. In order to reduce the turbulence generated by the fans and to obtain a uniform airflow, we install 32 mm plastic tubes to create settling chambers at the inflow and outflow. Just behind the inflow settling

chamber is the outlet of the gas source. As gas we use a mixture of ethanol vapor and air. At a distance of 0.3 m, 1.05 m, 1.25 m and 1.45 m from the source we place four Alphasense PID-AH gas sensors $S_1,\ldots,S_4$. We choose these photoionization detectors because they have a fast response time and do not suffer from drift. The analog sensor signals are sampled by a 16-bit analog-to-digital converter with about 400 Hz and recorded on a Raspberry Pi. The entire setup is closed with a lid during operation.

For the experimental evaluation, $N = 18$ experimental runs are analyzed. The index $k \in \{1,\ldots,N\}$ indicates the experimental run. In each experiment, the gas source is active for 0.1 s and the concentration at all gas sensors is recorded. Between the experimental runs, we always wait until the gas concentration at the sensors reaches zero again. Since we do not know the exact source signal and cannot assume a Dirac impulse, we use the gas sensor S_1 at 0.3 m as an artificial source (AS). In other words, we treat the signal recorded by sensor S_1 as our emitted source signal. The considered propagation channel from the AS to the other gas sensors is thus the distance to S_1. The unknown channel parameters (v, D) are estimated with sensor S_3 in each experimental run by

$$[v_k, D_k]^T = \underset{[v,D]^T, C}{\arg\max} \; \|s_{\mathrm{AS},k}(t) * \bar{c}(t) - s_{3,k}(t)\|^2, \qquad (14)$$

where $s_{\mathrm{AS},k}(t)$ is the signal of the AS, i.e., S_1, $\bar{c}(t)$ is the expected CIR depending on the distance to S_1, and $*$ is the convolution operator. Further, $s_{3,k}(t)$ is the observed signal at S_3 for experiment k. The estimated parameters v_k (mean: $0.59\,\mathrm{m\,s^{-1}}$, standard deviation (SD): $0.03\,\mathrm{m\,s^{-1}}$) and D_k (mean: $7.1\times10^{-3}\,\mathrm{m^2\,s^{-1}}$, SD: $3.6\times10^{-3}\,\mathrm{m^2\,s^{-1}}$) are very consistent across the different experimental runs.

The remaining sensors S_2 and S_4 are used for distance estimation. Since the presented estimators are based on the CIR, we have to recover the CIR $c_{i,k}(t)$ for $i \in \{2,4\}$ from the known AS signal $s_{\mathrm{AS},k}(t)$ and the observed concentration signal $s_{2,k}(t)$ and $s_{4,k}(t)$, respectively. The relation is given by

$$s_{i,k}(t) = s_{\mathrm{AS},k}(t) * c_{i,k}(t), \quad i \in \{2,4\}. \qquad (15)$$

Since information is lost during convolution, an unambiguous reconstruction is not possible. We use Wiener deconvolution to solve for the CIR $c_{i,k}(t)$. To do so, we assume that (15) is subject to additive white noise $n_k(t)$ with experimentally determined mean power spectral density $N_k(f) = 1000$. Together with the estimated channel parameters v_k and D_k, we are able to apply the presented ML (10) and ToPC (11) estimators.

The results of the different experimental runs (cf. Fig. 4) show that distance estimation from observations of a diffusive process is possible in practice with an accuracy on the scale of dm to cm (for distances $d \approx 1$ m). To compare the performance of the estimators in practice, further evaluations are needed. Also, the AoPC estimator has not been considered yet.

VI. Summary

In this paper, we derived the theoretical performance limit for distance estimators of diffusive processes. We calculated the CRB based on the channel model. The CRB was compared to a ML estimator that uses the arrival times of every particle and the channel model to estimate the distance. Furthermore, CRBs and estimators for ToPC and AoPC based distance estimation were determined. The CRBs were used to study the effect of channel parameters on the estimation performance. As expected, the simulation results showed that using all information yields the best estimation performance. To demonstrate that distance estimation is possible in practice, we conducted macro-scale experiments. The experiments have shown that dm to cm levels of accuracy are possible for distances $d \approx 1$ m. In future work, we plan to further improve our experimental setup and to evaluate the experimental results in more detail, including the AoPC estimator.

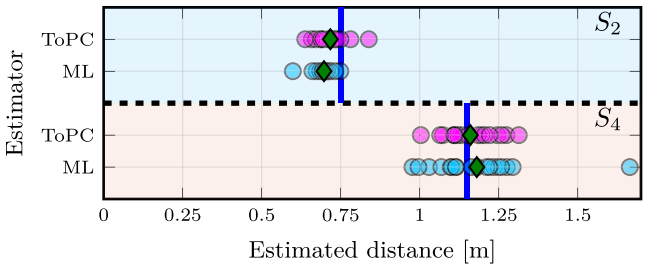

Fig. 4. Experiment results for the ML and ToPC estimator for the sensors S_2 ($d = 0.75$ m) and S_4 ($d = 1.15$ m) for $N = 18$ experimental runs. The green diamonds show the mean values of the estimated distances and the blue lines the ground truth.

References

[1] A. Francis, S. Li, C. Griffiths, and J. Sienz, "Gas source localization and mapping with mobile robots: A review," *J. Field Robot.*, vol. 39, no. 8, pp. 1341–1373, 2022.

[2] S. Bhattacharjee, M. Damrath, L. Stratmann, P. A. Hoeher, and F. Dressler, "Digital communication techniques in macroscopic air-based molecular communication," *IEEE Trans. Mol. Biol. Multi-Scale Commun.*, vol. 8, no. 4, pp. 276–291, Dec. 2022.

[3] N. Farsad, H. B. Yilmaz, A. Eckford, C.-B. Chae, and W. Guo, "A comprehensive survey of recent advancements in molecular communication," *IEEE Commun. Surveys Tuts.*, vol. 18, no. 3, pp. 1887–1919, 3rd Quart., 2016.

[4] M. J. Moore, T. Nakano, A. Enomoto, and T. Suda, "Measuring distance from single spike feedback signals in molecular communication," *IEEE Trans. Signal Process.*, vol. 60, no. 7, pp. 3576–3587, Jul. 2012.

[5] Y. Sun, M. Ito, and K. Sezaki, "An efficient distance measurement approach in diffusion-based molecular communication based on arrival time difference," in *Proc. 4th ACM Int. Conf. Nanoscale Comput. Commun.*, Sep. 2017, pp. 1–6.

[6] L. Lin, C. Yang, S. Ma, and M. Ma, "Parameter estimation of inverse Gaussian channel for diffusion-based molecular communication," in *Proc. IEEE Wirel. Commun. Netw. Conf.*, Apr. 2016, pp. 1–6.

[7] A. Noel, K. C. Cheung, and R. Schober, "Bounds on distance estimation via diffusive molecular communication," in *Proc. IEEE Glob. Commun. Conf.*, Dec. 2014, pp. 2813–2819.

[8] S. Kumar, "Nanomachine localization in a diffusive molecular communication system," *IEEE Syst. J.*, vol. 14, no. 2, pp. 3011–3014, Jun. 2020.

[9] V. Jamali, A. Ahmadzadeh, C. Jardin, H. Sticht, and R. Schober, "Channel estimation for diffusive molecular communications," *IEEE Trans. Commun.*, vol. 64, no. 10, pp. 4238–4252, Oct. 2016.

[10] S. M. Kay, *Fundamentals of Statistical Signal Processing, Volume I: Estimation Theory*. Hoboken, NJ, USA: Prentice Hall, 1993.

[11] T. Nakano, M. J. Moore, F. Wei, A. V. Vasilakos, and J. Shuai, "Molecular communication and networking: Opportunities and challenges," *IEEE Trans. Nanobiosci.*, vol. 11, no. 2, pp. 135–148, Jun. 2012.

[12] M. C. K. Tweedie, "Statistical properties of inverse Gaussian distributions. I," *Ann. Math. Statist.*, vol. 28, no. 2, pp. 362–377, Jun. 1957.

[13] M. Damrath and P. A. Hoeher, "Low-complexity adaptive threshold detection for molecular communication," *IEEE Trans. Nanobiosci.*, vol. 15, no. 3, pp. 200–208, Apr. 2016.
[14] S. Sand, W. Wang, and A. Dammann, "Cramér-Rao lower bounds for hybrid distance estimation schemes," in *Proc. IEEE Veh. Technol. Conf. (VTC Fall)*, 2012, pp. 1–5.

Fabio Broghammer received the M.Sc. degree in computer science from the Karlsruhe Institute of Technology, Germany, in 2021. In 2022, he joined the Institute of Communications and Navigation, German Aerospace Center as a Research Staff Member. His research interests include state estimation, swarm navigation, and sensing.

Siwei Zhang (Member, IEEE) received the B.Sc. degree in electrical engineering from Zhejiang University, China, in 2009, the M.Sc. degree in communication engineering from the Technical University of Munich, Germany, in 2011, and the Dr.-Ing. (Ph.D.) degree in electrical engineering from the University of Kiel, Germany, in 2020.

Since 2012, he has been a Researcher with the Institute of Communications and Navigation, German Aerospace Center, where he has been active in more than ten EU, German, and DLR projects in statistical signal processing in wireless communication and navigation. He is an External Lecturer with the Technical University of Munich and the University of Kiel. He is a recipient of the 2021 DLR Science Award and several Best Paper/Presentation Awards at international conferences, including 2015 and 2022 ION GNSS+, 2021 IEEE CCNC-RoboCom, and 2023 IEEE Aerospace Conference.

Thomas Wiedemann received the bachelor's and master's degrees from the Faculty of Mechanical Engineering, Technical University of Munich in 2012 and 2014, respectively, and the Ph.D. degree in computer science from the Center for Applied Autonomous Sensor Systems, Örebro University, Sweden, in 2021. He has been working as a Scientist with the Swarm Exploration Group, Institute of Communications and Navigation, German Aerospace Center since 2014. His research interests include multi-robot systems, robotic exploration, and gas source localization.

Peter A. Hoeher (Fellow, IEEE) received the Dipl.Ing. (M.Sc.) degree in electrical engineering from RWTH Aachen University, Aachen, Germany, in 1986, and the Dr.Ing. (Ph.D.) degree in electrical engineering from the University of Kaiserslautern, Kaiserslautern, Germany, in 1990. From 1986 to 1998, he was with German Aerospace Center, Oberpfaffenhofen, Germany. From 1991 to 1992, he was on leave with AT&T Bell Laboratories, Murray Hill, NJ, USA. Since 1998, he has been a Full Professor of Electrical and Information Engineering with Kiel University, Kiel, Germany. His research interests are in the general area of wireless communications and applied information theory. Since 2014, he has been a Fellow of the IEEE for contributions to decoding and detection that include reliability information.